Three-dimensional cellularized matrix supplemented with secretome enhances tissue regeneration in an incisional hernia repair model

Siufui Hendrawan[1,2]*, Olivia Marcelina[1], Astheria Eryani[3], Erwin Siahaan[4], and Hans U. Baer[1,5,6]

ABSTRACT

Present standard treatment for incisional hernia (IH) focuses on wound closure by providing mechanical reinforcement to the affected tissue, generally through the implantation of synthetic polypropylene (PP) mesh. However, PP mesh primarily functions to hold organs in place and does not actively stimulate intrinsic tissue regeneration. Meanwhile, in the aging population and in individuals with pre-existing complications, impaired wound healing and reduced elasticity increase the risk of hernia recurrence. In this study, we developed a three-dimensional cellularized implant with secretome (Sec) supplementation, aiming to promote tissue regeneration and the formation of a more mechanically robust scar in IH repair. The cellularized matrix (Cell/Matrix) was produced by seeding fibroblasts onto a three-dimensional collagen-coated poly-L-lactic acid matrix. Supplementation with Sec derived from human umbilical cord mesenchymal stem cells was performed to produce the Cell/Matrix+Sec implant. Implantation was performed in the sublay position (between muscle and peritoneal membrane), beneath an incisional cut at the midline abdomen of Wistar rats to mimic IH repair. Rats with no implant (Sham) served as the control group, while others received PP mesh (Mesh), an acellularized matrix (Matrix), Cell/Matrix, and Cell/Matrix+Sec implants. At 2 months post-implantation, abdominal tissue samples extracted from the Cell/Matrix+Sec implant group exhibited the greatest biomechanical strength, accompanied by a higher collagen type I/III ratio, neovascularization count, α-smooth muscle actin-positive vessels, and formation of neuron bundles. Meanwhile, Sham and Mesh groups displayed the lowest values in all parameters, respectively. Despite having lower mechanical strength compared with PP mesh, implantation of the cellularized matrix resulted in better muscle tissue integrity and maturation. Hence, these findings highlight the potential of Cell/Matrix+Sec as a novel adjuvant implant to complement the present standard approach to hernia repair, which lacks regenerative capacities.

Keywords:
Abdominal tensile strength; Collagen ratio; Incisional hernia; Poly-L-lactic acid cellularized matrix; Secretome; Human umbilical cord-derived mesenchymal stem cells

***Corresponding author:**
Siufui Hendrawan,
siufui@fk.untar.ac.id

How to cite this article:
Hendrawan S, Marcelina O, Eryani A, Siahaan E, Baer HU. Three-dimensional cellularized matrix supplemented with secretome enhances tissue regeneration in an incisional hernia repair model. *Biomater Transl.* **2025**.

doi: 10.12336/bmt.25.00041

1. Introduction

Incisional hernia (IH) is a post-operative complication following abdominal surgery, characterized by incomplete healing of the abdominal wall that fails to hold organs in place. Repair techniques for IH have been widely established, mainly through the implantation of mesh, either through open surgery or minimally invasive laparoscopy.[1,2] Nevertheless, present standard strategies still result in relatively high recurrence rates and complications, such as adhesion to adjacent tissue, seroma formation,

and mesh rupture.[1-3] While the incidence rate of IH is reported to be as high as 10.3% within 2 years post-abdominal surgery,[3] the recurrence rate following hernia repair can reach 27% and tends to increase over longer observation periods.[4,5]

Although the pathophysiology of IH is yet to be fully elucidated, one major indicator is a homeostatic disturbance in the extracellular matrix (ECM). Previous findings suggest that fibroblasts with altered phenotypic functions are markedly present in IH tissue and are responsible for synthesizing an abnormal ECM composition. In this state, transdifferentiation of immature fibroblasts into myofibroblasts is suppressed, as shown by the increased presence of $CD34^+$ fibroblasts, a surface marker for undifferentiated fibroblasts. Meanwhile, α-smooth muscle actin (α-SMA), the myofibroblast biomarker, is reduced in IH.[6] Instead of accumulating mechanically "strong" collagen type I (COL1), these immature fibroblasts produce excessive mechanically "weak" collagen type III (COL3), resulting in a lower ratio of COL1:COL3 found in biopsies of patients with recurrent IH. This abnormal ECM composition reduces tissue tensile strength, rendering it prone to dehiscence.[6,7]

Synthetic polypropylene (PP) mesh, a sheet of non-absorbable material, is commonly utilized for hernia repair due to its low cost and high mechanical strength. Despite being the longstanding gold standard, PP mesh is still associated with post-operative complications, such as inflammation, infection, and chronic pain-related discomfort.[8,9] In more severe cases of complications, a secondary surgery may be required to remove the mesh, consequently causing additional tissue damage.[1] Therefore, the present trend focuses on developing biocompatible constructs that can effectively integrate with host tissue without inducing a foreign body response or inflammation. Ultimately, the construct should be able to induce intrinsic regeneration, a critical aspect lacking in PP mesh implantation.[10]

To meet the clinical demand for devices capable of inducing tissue regeneration, various smart-engineered matrix scaffolds have been developed as alternatives to conventional prosthetic meshes, such as electrospun membranes, hydrogel patches, and other three-dimensional (3D) scaffolds. Biological meshes, such as collagen, although possessing weaker biomechanical properties, offer advantages over synthetic non-absorbable meshes in stimulating muscle regeneration without inducing an inflammatory response.[11] Therefore, coating synthetic mesh with biological agents is another strategy to improve its biocompatibility.[12] In our previous study, we developed a 3D cellularized matrix as a potential treatment for IH.[13] The implant is composed of a biodegradable cell–carrier matrix made of poly-L-lactic acid (PLLA) coated with collagen and seeded with allogeneic dermal fibroblasts. Moreover, this construct is supplemented with secretome (Sec) derived from human umbilical cord mesenchymal stem cells (hUC-MSCs).[13]

The Sec of hUC-MSCs is a cell-free product with several advantages: a lower risk of immune reaction, ease of acquisition, and proven regenerative therapeutic effects. Our previous findings indicate that various growth factors contained in the Sec can promote fibroblast migration and enhance their function in collagen production.[13-15] Furthermore, in clinical settings, we have observed that Sec administration can accelerate chronic wound healing, including diabetic wounds and leprosy.[16,17] Early evidence from a rat model study demonstrated that tissue implanted with a 3D cellularized scaffold contains the highest quantity of fibroblasts around the hernia repair site, compared with tissue implanted with mesh or an acellularized scaffold matrix. Moreover, tissue sections from the Sec -supplemented cellularized matrix exhibit mature granulated tissue with complete differentiation, closely resembling normal tissue sections.[13]

Therefore, in this study, we aim to investigate the effect of the 3D cellularized matrix with Sec supplementation on abdominal muscle strength by performing a tensile pull test on abdominal tissue post-hernia repair in rats. We also assess the ratio of COL1:COL3, neovascularization, and markers of neuron bundles and muscularization. To our knowledge, this study is the first to develop a 3D biodegradable cellularized matrix with Sec supplementation capable of carrying cells and inducing tissue regeneration to strengthen damaged areas and reduce the likelihood of recurrence.

2. Methods

2.1. Fabrication of the three-dimensional PLLA collagen-coated (PLLA/CC) scaffold

The 3D matrix was fabricated from the synthetic polymer PLLA (PLA Resomer® L206S, Evonik, United States [USA]) using a salt-leaching process.[12,18] The PLLA scaffold had >90% porosity (pore diameter: 355–425 μm) and was subsequently cut into rectangular shapes measuring 1 cm × 2 cm with a thickness of 0.2 cm (**Figure 1**). To construct the PLLA/CC matrix, the matrix was immersed in a 0.5% w/v AteloCell® bovine collagen solution (KOKEN®, Japan) and subjected to reduced pressure to ensure that the collagen penetrated and coated all pores.[19,20] To drain the excess collagen, the matrix was placed onto a 100 μm cell-strainer and centrifuged at 2,000 × g for 10 min. A freeze-drying process was then performed under vacuum (<5 Pa) for 24 h (EYELA FDU-2200, Eyela, Japan). To improve the biocompatibility and hydrophilicity of the material, the PLLA/CC matrix was treated with plasma activation, which involved the addition of oxygenated functional groups onto the material surface, thereby modifying its hydrophobicity, using a custom-made plasma machine (Diener Electronic GmbH, Germany). Sterilization was performed using 30% hydrogen peroxide (H_2O_2) (Merck, Sigma-Aldrich, USA) at 30A for at least 1 h in the plasma machine.[12]

[1]Tarumanagara Human Cell Technology Laboratory, Faculty of Medicine, Tarumanagara University, Jakarta, Indonesia; [2]Department of Biochemistry and Molecular Biology, Faculty of Medicine, Tarumanagara University, Jakarta, Indonesia; [3]Department of Histology, Faculty of Military Medicine, Indonesia Defense University, Bogor, West Java, Indonesia; [4]Department of Mechanical Engineering, Faculty of Engineering, Tarumanagara University, Jakarta, Indonesia; [5]Baermed Tissue Engineering Limited, Freienbach, Switzerland; [6]Department of Visceral and Transplantation Surgery, Faculty of Medicine, University of Bern, Bern, Switzerland

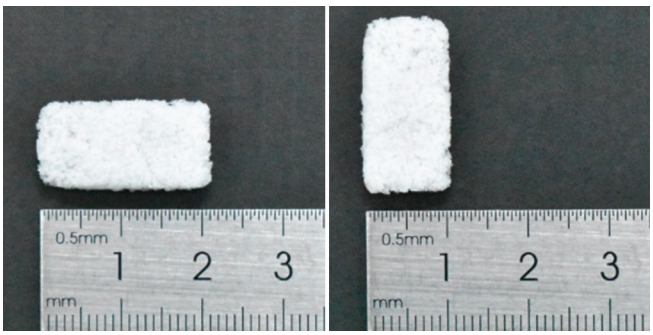

Figure 1. Three-dimensional matrix of collagen-coated poly-L-lactic acid. The matrix was shaped into rectangular shapes measuring 1 cm × 2 cm.

2.2. Preparation of human umbilical cord-derived mesenchymal stem cell Sec

Sec was obtained from hUC-MSCs using methods established in a previous study,[14] and the procedure was approved by the Human Research Ethics Committee of Tarumanagara University (UTHREC No. PPZ20192062). In brief, fresh hUC was obtained from a healthy donor with parental consent, followed by processing and seeding the isolated MSCs into T75 flasks. The tissue was cultured in Minimum Essential Medium-α (Gibco, Life Technologies, USA) containing 20% fetal bovine serum (Gibco, USA) and 1% antibiotic–antimycotic (Sigma-Aldrich, USA). hUC-MSCs were expanded and cultured through several passages. At 80% confluency, hUC-MSCs were pre-treated with serum starvation and incubated under hypoxic conditions (5% O_2) in a CO_2 incubator with an O_2 controller (Forma™ Steri-Cycle™ i160 Dual CO_2 incubator, Thermo Fisher Scientific, USA). The culture medium was subsequently collected and separated from any remaining cells through centrifugation. Finally, the Sec was filtered through a 0.22 μm filter membrane to obtain a sterile, cell-free Sec, which was stored in a deep freezer at −80°C.

2.3. Stability test of human umbilical cord-derived mesenchymal stem cell Sec

Total protein content of the hUC-MSC Sec was quantified using the bicinchoninic acid assay kit (Pierce™ BCA Protein Assay Kit, Thermo Fisher Scientific, USA), following the instructions provided in the kit. In addition to total protein measurement, the concentrations of two key pro-angiogenic factors were also measured: vascular endothelial growth factor (VEGF) (Human VEGF DuoSet, R&D Systems, USA) and basic fibroblast growth factor (bFGF) (Human DuoSet bFGF, R&D Systems, USA), using enzyme-linked immunosorbent assay. To assess protein and growth factor stability, the Sec was stored at −80°C and analyzed at the following time points: fresh, 2, 4, 6, and 8 weeks. Results were expressed as the percentage of preserved levels at each time point, relative to the concentration at the fresh condition.

2.4. Production of the three-dimensional cellularized matrix with Sec supplementation

Production of fibroblast-seeded matrix (Cell/Matrix) was performed by seeding 2 × 10^6 primary rat dermal fibroblasts onto each PLLA/CC matrix. Fibroblasts were isolated following the established protocol in a previous study.[13] The fibroblast-seeded matrix was cultivated in Dulbecco's Modified Eagle's Medium (Sigma-Aldrich, USA) containing 10% fetal bovine serum, 1% sodium pyruvate (Sigma-Aldrich, USA), 1% 4-(2-hydroxyethyl) piperazine-1-ethanesulfonic acid (Sigma-Aldrich, USA), and 1% of antibiotic–antimycotic. For the group supplemented with Sec (Cell/Matrix+Sec), Sec was added to the culture medium (final concentration: 1% v/v) during the seeding process. After 24 h of seeding, the cellularized matrix was ready for implantation.

2.5. Evaluation of plasma activation and hydrogen peroxide sterilization of the matrix

Cell–matrix adhesion following plasma activation was assessed using the Cell Counting Kit-8 (CCK-8) (Sigma-Aldrich, USA) assay, according to the manufacturer's instructions. To evaluate the effectiveness of plasma activation, two groups were compared: (i) PLLA/CC matrix treated with both plasma activation and H_2O_2 sterilization, and (ii) PLLA/CC matrix treated with H_2O_2 sterilization alone (without plasma activation). Primary rat dermal fibroblasts were seeded onto the matrices as previously described in Section 2.4. After 24 h of incubation, each matrix was transferred to a new culture plate containing a working solution (culture medium: CCK-8 solution ratio, 10:1). Samples were incubated for 4 h at 37°C with 5% CO_2, and the absorbance was measured at 450 nm. As a control, an equal number of cells were seeded on a two-dimensional (2D) culture plate. Results were expressed as the fold change of viable, adherent cells compared with the 2D control, which was normalized to 1. A sterility test was conducted following H_2O_2 sterilization by subjecting each matrix to CASO agar, CASO broth, thioglycolate broth, and Saboraud broth (Sigma-Aldrich, USA), to detect the presence of aerobic and anaerobic bacteria as well as fungal growth.

2.6. Scanning electron microscopy

The presence and morphology of fibroblasts in the 3D matrix were visualized through scanning electron microscopy. The matrix was pre-treated before imaging following the method established in a previous study.[12] The sample was fixed in 3% glutaraldehyde for two hours and dehydrated in ethanol with a serial concentration gradient up to 100%. Subsequently, the sample was completely dried using the chemical agent hexamethyldisilane (Sigma-Aldrich, USA) and air-dried under a fume hood for 24 h at room temperature. Energy-dispersive spectroscopy analysis was performed on the surface of the 3D matrix to detect the elemental content. Imaging was performed using a Quattro S (Thermo Fisher Scientific, USA) at the Integrated Laboratory of Bioproduct, National Research and Innovation Agency, Banten, Indonesia.

2.7. Animal study

Male Wistar rats aged 8–10 weeks (n = 25) were acquired from PT Bio Farma, Indonesia. The animal study was conducted at the Tarumanagara Human Cell Technology Laboratory, Faculty of Medicine, Tarumanagara University, Jakarta, Indonesia, with approval from the Institutional Animal Care

and Use Committee (IACUC) of Tarumanagara University (IACUC No. 017.KEPH/UPPM/FK/VI/2023). The number of animals used in this study was calculated through the analysis of variance (ANOVA) Research Equation formula, while considering the 3Rs principle (Replacement, Reduction, and Refinement). Anesthesia was induced through intraperitoneal injection of 10% ketamine at a dose of 40–80 mg/kg body weight (Kepro, Netherlands) and 2% xylazine at a dose of 5–10 mg/kg body weight (Interchemie, Netherlands).

The hernia repair model was performed based on the method established in our previous study, with slight modifications.[13] Rats were randomly assigned into five groups ($n = 5$ per group) based on the implant received during hernia repair: (i) Sham (without an implant); (ii) Mesh (implanted with a synthetic monofilament PP mesh of 1 cm × 2 cm [Trulene, India]); (iii) Matrix (implanted with an acellularized PLLA/CC matrix); (iv) Cell/Matrix (implanted with a cellularized matrix); and (v) Cell/Matrix+Sec (implanted with a cellularized matrix with Sec supplementation). From each group, three rats were subjected to biomechanical tensile pull testing, while the remaining rats ($n = 2$ per group) were analyzed for histological assessment.

Briefly, a 1.8 cm midline laparotomy was carefully created across the abdominal muscle without interfering with the peritoneal membrane. Hernia repair was performed by placing the implant between the muscle and peritoneal membrane (sublay implantation, retromuscular position) according to each group (**Figure 2**). Finally, both the abdominal muscle and skin were closed with absorbable 4-0 Vicryl suture (W9386, Ethicon, USA) and covered with Hypafix® (Essity, Sweden). Rats were kept for 2 months until they were sacrificed for further biomechanical tensile pull testing and histological analysis.

2.8. Biomechanical test

Two months after the hernia repair procedure, the strength of the abdominal muscle at the implantation site was determined through a uniaxial tensile pull test on a strip of muscle tissue containing the implant.[21] Briefly, the abdominal muscle measuring 4 cm × 6 cm at the operation site was collected and stored in physiological saline for immediate tensile testing. For the tensile pull test, the specimen was oriented along the transverse axis and fixed onto the top and bottom grips made of customized rubber (**Figure 3**). The test was carried out using a custom-made universal testing instrument with a dynamic force processor (Unipulse F381A, Unipulse, Japan), applying a load at a uniform speed of 400 rpm until the tissue ruptured. The maximum load borne by each specimen was recorded in Newtons (N).

2.9. Histological analysis

For histological analysis, a specimen of abdominal muscle was fixed in 4% paraformaldehyde and embedded in a paraffin block for further staining. The staining and histopathological assessments were performed at the Pathology and Anatomy Laboratory, Primate Research Centre, Bogor Agricultural University. Hematoxylin and eosin (H&E) staining was performed to observe neovascularization within the scar tissue. The total collagen area was determined through Sirius Red staining (Picro-Sirius Red ab246832, Abcam, United Kingdom) by measuring the positively stained area across the whole abdominal tissue specimen. To establish the ratio between COL1 and COL3 (COL1:COL3), the specimen was examined under polarized light using a light microscope (Olympus CX23, Olympus, Japan) equipped with custom polarizing and analyzer filters. COL1 was indicated by a network stained reddish-orange, while COL3 was

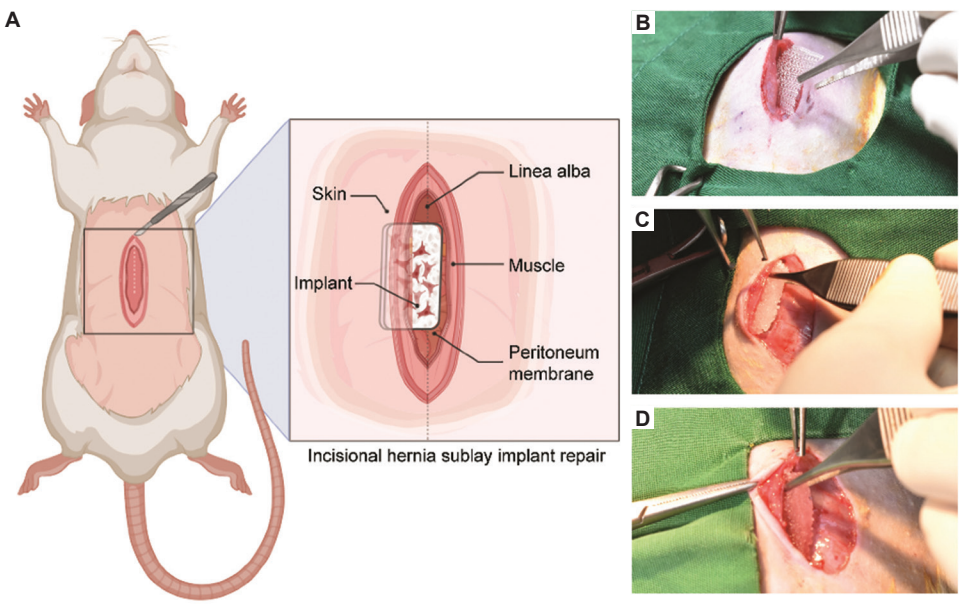

Figure 2. Schematic diagram of the hernia sublay implant repair technique. (A) The implant is positioned between the abdominal muscle and the peritoneal membrane. Created in BioRender. Lab, T. (2025) https://BioRender.com/tufoyfz. (B-D) Representative images of hernia repair using: (B) mesh, (C) acellular poly-L-lactic acid matrix, and (D) cellularized matrix.

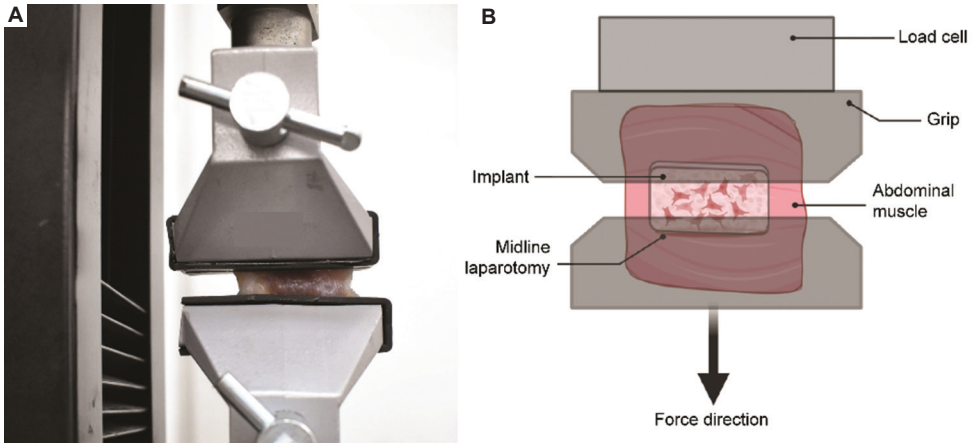

Figure 3. Biomechanical tensile pull test to evaluate the strength of the abdominal muscle with the implant. (A) Photograph of the tensile pull test setup for an abdominal muscle strip. (B) Schematic diagram of the experimental setup. Specimens were secured in the top and bottom grips and pulled downward at a constant speed of 400 rpm. Created in BioRender. Lab, T. (2025) https://BioRender.com/a81bjeu.

shown in yellowish-green birefringence. The area densities corresponding to each type of collagen were quantified using ImageJ software (National Institutes of Health, USA), and the ratio between COL1 and COL3 was determined.[22] Immunohistochemical staining was also conducted for α-SMA (ab_2572996, Thermo Fisher Scientific, USA) and neuron-specific enolase (NSE) (ab_2544928, Thermo Fisher Scientific, USA).[10] Five microscopic fields adjacent to the midline laparotomy and implant site were counted from each section at ×200 magnification.

2.10. Statistical analysis

Results were expressed as mean ± standard deviation. The test of normality was performed using the Shapiro–Wilk test. The *in vivo* biomechanical test was assessed using a one-way ANOVA (IBM SPSS Statistics, IBM Corp., USA). Differences were considered statistically significant at $p<0.05$ and highly significant at $p<0.01$.

3. Results

3.1. Biocompatibility of the three-dimensional cellularized matrix

Different types of 3D matrices are available for cell delivery, with their main objective being to mimic the tissue-like microenvironment.[23] Herein, a 3D matrix was developed to serve as a carrier for cells, particularly fibroblasts, to facilitate collagen production and thereby promote the formation of stronger connective tissues and enhance wound healing. This 3D matrix was made of PLLA through particulate leaching with salt particles of 355–425 μm in diameter to generate pores for cell permeation and nutrient transfer.[23] This PLLA matrix was then pre-coated with a nanometer-thick layer of collagen to enable fibroblast adhesion.[12] Furthermore, oxygen plasma activation treatment was employed to enhance the hydrophilicity of the matrix, overcoming the inherently hydrophobic nature of PLLA.

As shown in **Figure 4A**, while collagen coating enabled cell adhesion within the matrix, plasma activation further improved the level of adhesion, approaching the value obtained in the 2D well-plate control. To sterilize the PLLA/CC matrix without compromising the collagen coating, low-temperature sterilization using H_2O_2 vapor was performed. This method effectively rendered the PLLA/CC matrix sterile, with no bacterial or fungal growth observed in CASO agar/broth, thioglycolate broth, and Saboraud broth (**Figure 4B**).

When analyzed through energy-dispersive spectroscopy, the resulting 3D matrix was composed of only carbon and oxygen atoms (**Figure 4C**). Scanning electron microscopy analysis revealed the porous morphology of the acellularized matrix (**Figure 4D**). When seeded with fibroblasts and supplemented with Sec, robust fibroblast colonization throughout the matrix was observed (**Figure 4E**). These findings indicate that the designed 3D matrix is a promising cell carrier for facilitating fibroblasts' growth. Furthermore, an *in vivo* study was performed to evaluate the effectiveness of a 3D cellularized matrix in promoting hernia repair.

3.2. Three-dimensional cellularized matrix with Sec promotes functional tissue regeneration in hernia repair

Extensive studies have confirmed the role of Sec derived from hUC-MSCs in tissue regeneration by stimulating cellular growth and function.[13-15] Previously, we confirmed the robust content of pro-angiogenic factors in hUC-MSC Sec, such as VEGF, bFGF, procollagen-I, and hepatocyte growth factor. In this study, the Sec contained a relatively high level of total protein (1879 μg/mL). Under −80°C storage, the protein level remained stable for 2 weeks and declined by approximately 30% after 8 weeks (**Figure 5A**). Similarly, VEGF levels decreased at a comparable rate, whereas bFGF showed faster degradation, with a 53% decrease by week 8 (**Figure 5B**). This finding suggests that fresh or short-term stored Sec should be used for maximal therapeutic effect.

While developing the cellularized matrix implant, we supplemented hUC-MSC Sec during the cell culture process to maximize fibroblasts' capacity for collagen production. Implantation of this construct was expected to induce more complete and stronger scar tissue formation during hernia repair. Two months after implantation, critical features of

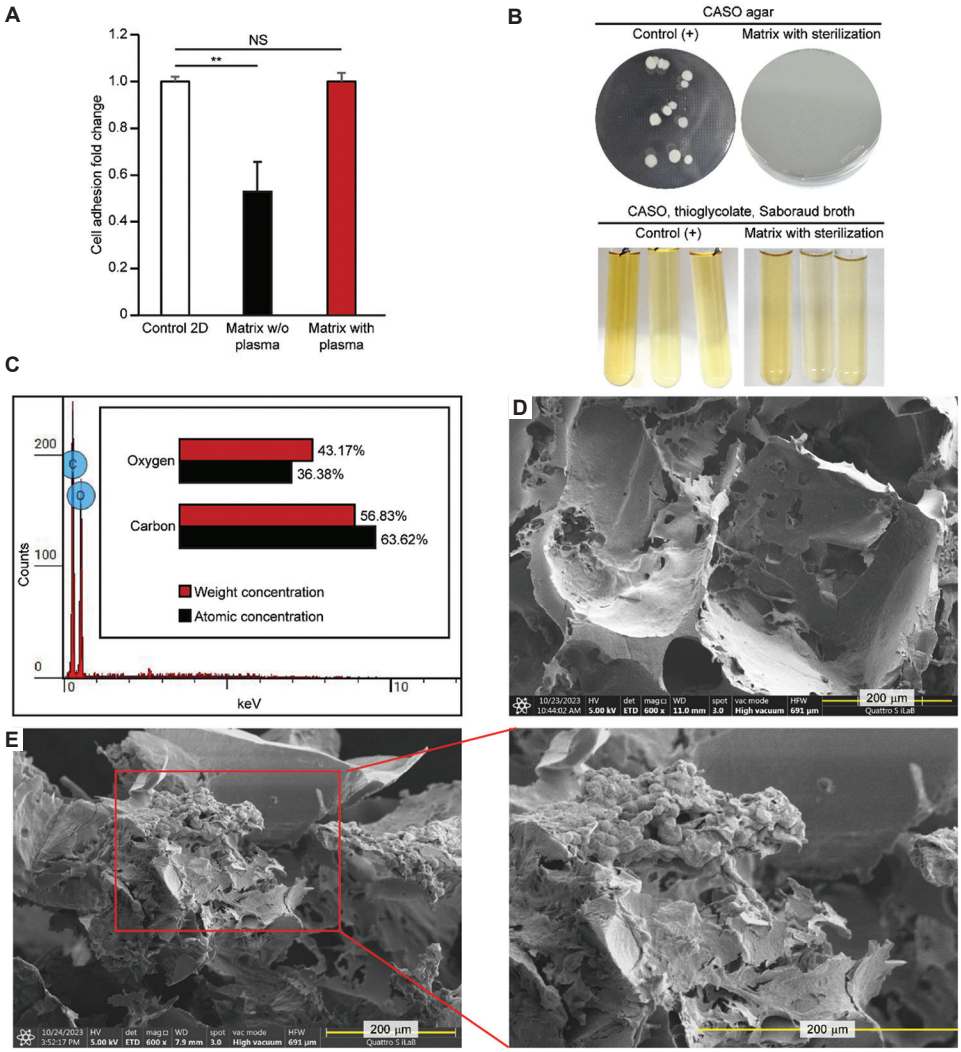

Figure 4. Biocompatibility, sterility, and elemental analysis of the 3D PLLA/CC matrix. (A) The effect of plasma activation on cell–matrix adherence, evaluated using the Cell Counting Kit-8 assay ($n = 3$). "Control 2D" represents fibroblasts seeded on a 2D culture plate, "Matrix w/o plasma" signifies fibroblasts seeded on a PLLA/CC matrix without plasma activation, and "Matrix with plasma" indicates fibroblasts seeded on a PLLA/CC matrix with plasma activation. Data are shown as mean ± standard deviation, with a double asterisk (**) indicating statistical significance at $p<0.01$, compared with "Control 2D." (B) Sterility test of the matrix following low-temperature hydrogen peroxide sterilization, performed on CASO agar, CASO broth, thioglycolate broth, and Saboraud broth. (C) Energy dispersive spectroscopy analysis of the 3D matrix. Scanning electron microscopy image of (D) the acellularized matrix and (E) the cellularized 3D matrix with secretome supplementation; red box indicates adhered fibroblasts, magnified in the right panel (magnification: ×600; scale bar: 200 µm).
Abbreviations: 2D: Two-dimensional; 3D: Three-dimensional; NS: Not significant; PLLA/CC: Collagen-coated poly-L-lactic acid; w/o: Without.

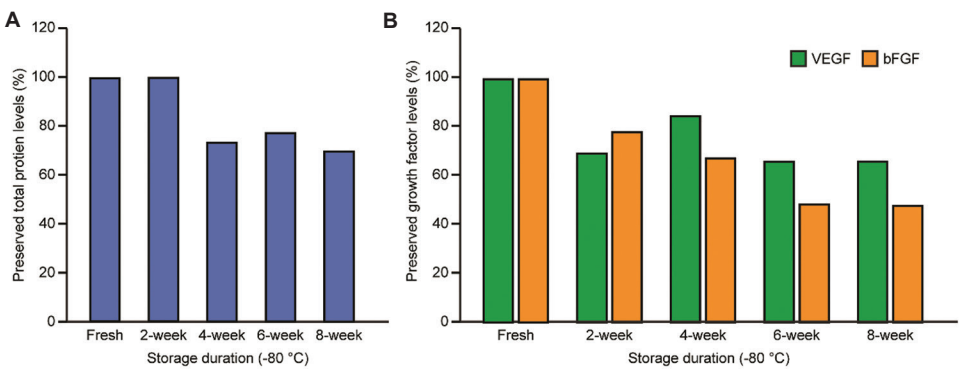

Figure 5. Stability of the human umbilical cord-derived mesenchymal stem cell secretome stored at −80□ for 2, 4, 6, and 8 weeks. (A) Total protein levels in the secretome, measured using the bicinchoninic acid assay. (B) Levels of the pro-angiogenic factors VEGF and bFGF in the secretome, quantified by enzyme-linked immunosorbent assay.
Abbreviations: bFGF: Basic fibroblast growth factor; VEGF: Vascular endothelial growth factor.

functional tissue regeneration *in vivo* were observed, including neovascularization, muscularization, and neurogenesis.

After the hernia sublay implant repair, abdominal muscle samples from the implantation area were collected and subjected to histological staining. Neovascularization assessed through H&E staining revealed that the Cell/Matrix+Sec group exhibited the greatest neovascularization, followed by the Cell/Matrix and Matrix groups, although no statistical analysis was performed due to the low sample number (**Figure 6A** and **D**). In contrast, neovascularization counts remained lower in the Sham and Mesh groups.

The Cell/Matrix+Sec group also demonstrated the highest count of α-SMA-positive vessels and NSE-positive neuron bundles (**Figure 6B** and **C**). The Sham group displayed the lowest counts of smooth muscle vasculatures and neuron bundles, while the Mesh and Matrix groups showed similar results (**Figure 6E** and **F**). These findings indicate that not only did the Cell/Matrix+Sec group have greater vessel formation, but these vessels were also enclosed by smooth muscle cells. Altogether, these findings indicate the regenerative effect of the Cell/Matrix+Sec implant during hernia repair, as evidenced by the formation of complete vessels and neuron bundles.

3.3. Three-dimensional cellularized matrix with Sec enhances COL1/III ratio in hernia repair

The ratio between COL1 and COL3 (COL1:COL3) is an important marker in hernia repair, as it reflects the mechanical integrity of the affected tissue. COL1 is mechanically stronger than COL3, which has a fibrous phenotype that is stiffer and thicker in diameter. Therefore, a lower COL1:COL3 ratio is associated with poor wound healing in hernia repair. When analyzed under polarized light, COL1 and COL3 can be differentiated due to their differences in birefringence, thickness, and fiber organization.[24,25]

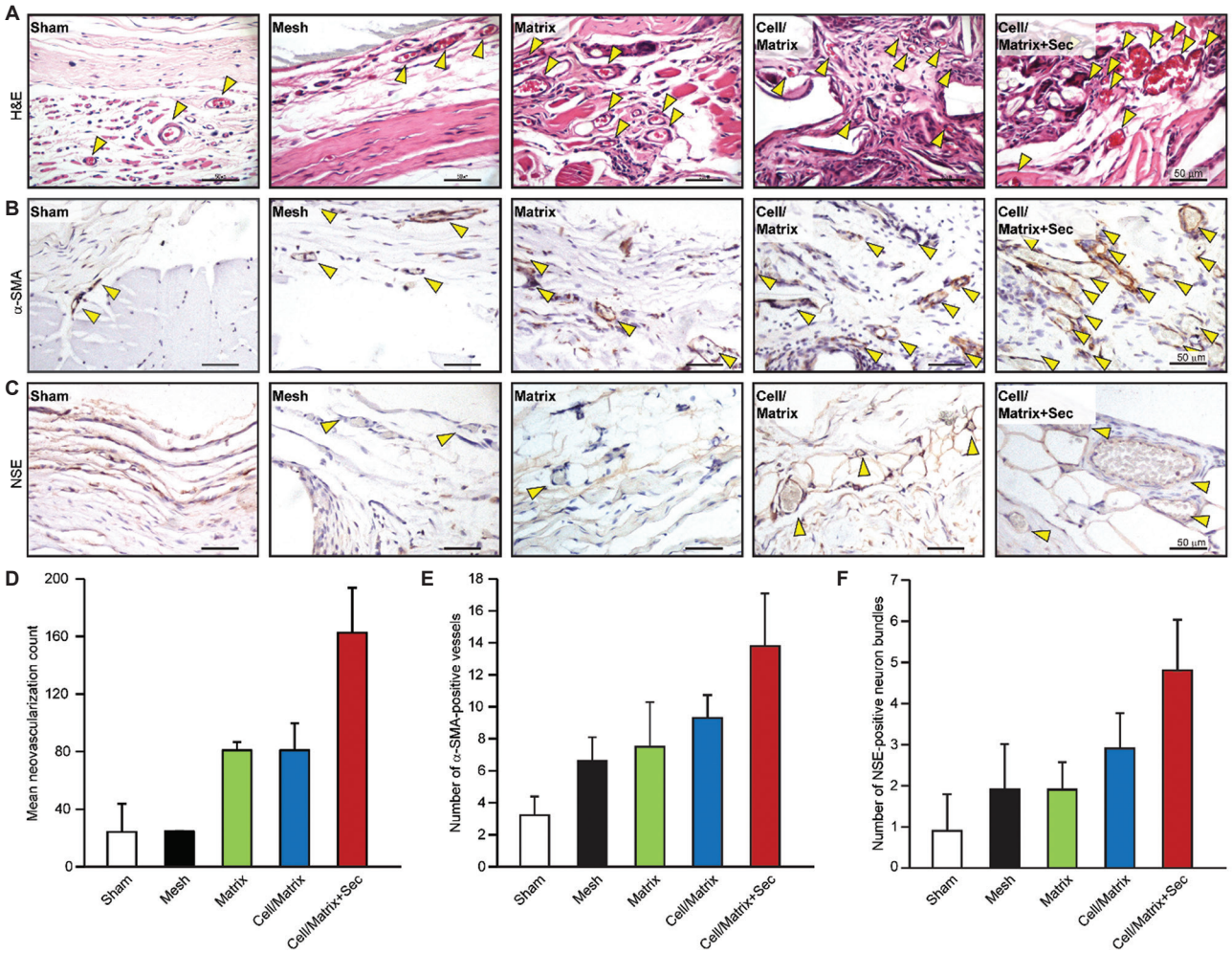

Figure 6. Neovascularization, smooth muscle, and neurogenesis development in abdominal muscle tissue 2 months after hernia repair. Representative images of (A) neovascularization bundles, (B) α-SMA-positive vessels, and (C) NSE-positive neuron bundles, indicated by yellow triangles (magnification: ×200; scale bar: 50 μm). Quantification of the mean (D) neovascularization count, (E) number of α-SMA-positive vessels, and (F) number of NSE-positive neuron bundles, evaluated using hematoxylin and eosin staining. The H&E staining only accounts the neovascularization count, while the other were stained with α-SMA and NSE antibodies, respectively. Mean numbers were generated from counts of five field views (n = 2). "Sham" indicates hernia repair without an implant; "Mesh" represents hernia repair using a mesh; "Matrix" signifies hernia repair with an acellularized 3D PLLA matrix; "Cell/Matrix" indicates hernia repair using a cellularized 3D PLLA matrix; and "Cell/Matrix+Sec" represents hernia repair using a secretome-supplemented Cell/Matrix.
Abbreviations: 3D: Three-dimensional; α-SMA: α-Smooth muscle actin; NSE: Neuron-specific enolase; PLLA: Poly-L-lactic acid.

Two months after hernia repair, Sirius Red staining indicated that the Cell/Matrix+Sec group exhibited the highest mean total collagen-positive area, followed by the Cell/Matrix and Matrix groups. In contrast, the Sham and Mesh groups exhibited significantly lower collagen-positive areas (**Table 1**).

A similar trend was observed when COL1 and COL3 were distinguished using a polarized microscope. Abdominal tissue from the Cell/Matrix+Sec group demonstrated the highest COL1:COL3 ratio, followed by the Cell/Matrix and Matrix groups. In contrast, tissue from the Sham group exhibited a thinned muscle layer around the midline laparotomy. Collagen deposition surrounding the midline laparotomy in the Mesh group was dominated by yellowish-green birefringence, indicating the presence of COL3. These findings correspond to the lower total collagen content in the Sham and Mesh groups, along with their poor COL1:COL3 ratios (**Figure 7**). Collectively, these results suggest that implantation of the Cell/Matrix+Sec promotes greater total collagen deposition and a higher ratio of COL1:COL3, although the low sample size precluded statistical analysis.

3.4. Three-dimensional cellularized matrix enhances tissue strength in hernia repair

The mechanical strength of each abdominal muscle tissue was evaluated through tensile pull testing. In this procedure, a load was applied to each tissue strip at a constant speed, and the maximum force borne by each specimen before rupture was recorded. The findings revealed that the abdominal muscle implanted with Cell/Matrix+Sec could withstand the highest maximum force (64.39 ± 0.67 N), followed by Cell/Matrix (55.72 ± 7.83 N), although the difference was not statistically significant compared with the Mesh group (52.16 ± 3.05 N). Compared with the Sham group (40.24 ± 7.04 N), the Cell/Matrix+Sec group exhibited significantly greater abdominal muscle strength (p<0.01). The Matrix and Mesh groups also demonstrated greater endurance in withstanding forces compared with the Sham group, although these differences were not statistically significant (**Figure 8**). These findings indicate that implantation of Matrix and Mesh produces comparable abdominal tissue strength, while cellularized matrix provides greater enhancement, particularly when supplemented with the Sec of hUC-MSCs.

Table 1. Mean collagen-positive area and collagen type I/III ratio at the implant area

Group (n=2)	Mean collagen-positive area (μm²)	Ratio of collagen type I/III
Sham	12,483±4,879	2.21±0.40
Mesh	15,021±9,737	3.59±0.21
Matrix	3,220,166±4,528,736	6.33±5.62
Cell/Matrix	5,296,480±879,171	6.79±0.59
Cell/Matrix+Sec	6,747,035±1,581,287	10.14±1.65

4. Discussion

To date, the incidence and recurrence rates of IH remain considerably high, especially in the aging population and in patients with pre-existing complications.[3-5] Loss of tissue elasticity and compromised wound healing in this subset further impede the formation of a fully functional abdominal wall with load-bearing capacity.[26] As the standard therapy, reinforcement of static mesh still presents a set of drawbacks, as it tends to induce undesirable immunologic responses and the formation of stiff scar tissue. This can lead to implant shrinkage and subsequent de-coverage of the hernia injury.[27] Therefore, recent advances in hernia repair have shifted from the use of 2D conventional meshes toward the development of smart regenerative scaffolds, emphasizing the need for a regenerative device to reduce recurrence and complication risks.[10,28]

In this study, we utilized a 3D cellularized matrix made of PLLA/CC for IH repair. PLLA is a biocompatible, United States

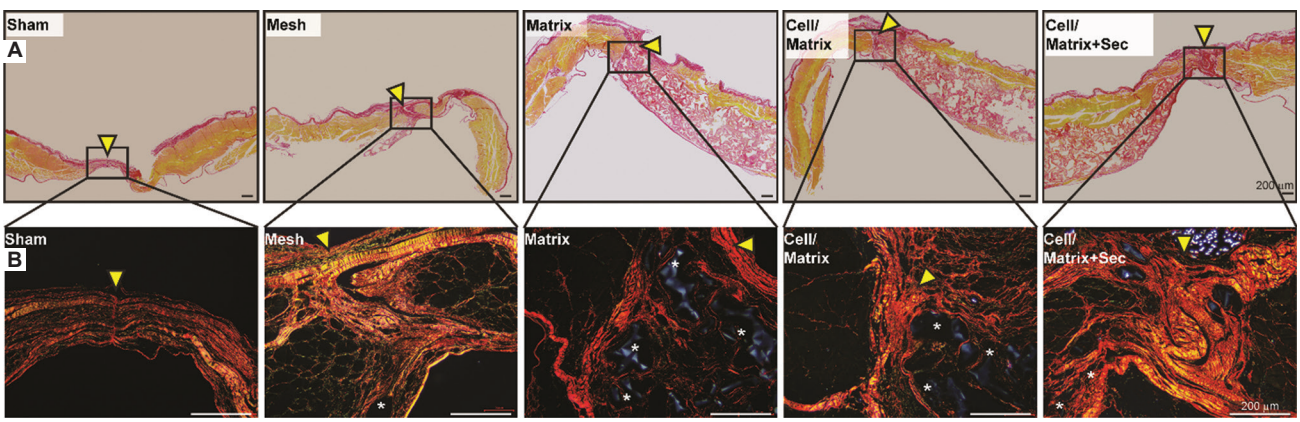

Figure 7. Collagen distribution in abdominal muscle tissue 2 months after hernia repair, visualized by Sirius Red staining. (A) Total collagen distribution (red staining) observed under a light microscope (magnification: ×100; scale bar: 200 μm). (B) Distribution of COL1 (reddish-orange) and COL3 (yellowish-green birefringence) around the incision and implant area, visualized under polarized light (magnification: ×100; scale bar: 200 μm). Yellow triangles indicate the incision area, black boxes mark the focus area shown at ×100 magnification in the B panels, and a white asterisk (*) denotes the implant. "Sham" represents hernia repair without an implant; "Mesh" indicates hernia repair using a mesh; "Matrix" signifies hernia repair with an acellularized 3D PLLA matrix; "Cell/Matrix" represents hernia repair using a cellularized 3D PLLA matrix; and "Cell/Matrix+Sec" indicates hernia repair using secretome-supplemented Cell/Matrix.
Abbreviations: 3D: Three-dimensional; COL1: Collagen type I; COL3: Collagen type III; PLLA: Poly-L-lactic acid.

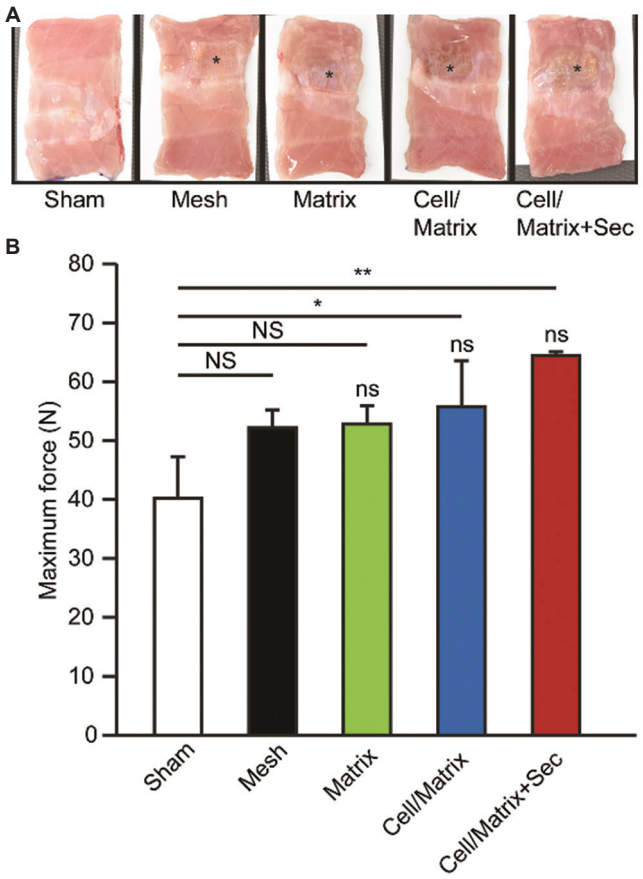

Figure 8. Biomechanical strength of abdominal muscle tissue 2 months after hernia repair. (A) Representative images of abdominal tissue post-hernia repair in the respective groups. Black asterisk (*) denotes the remaining implant. (B) Maximum force borne by the abdominal tissue before rupture, measured using a tensile pull test (n = 3). Data are shown as the mean ± standard deviation. Statistical significance is indicated as follows: "NS," single asterisk (*), and double asterisk (**) indicate not significant, p<0.05, and p<0.01, respectively, when compared to the "Sham" group, whereas "ns" indicates not significant when compared to the "Mesh" group. "Sham" represents hernia repair without an implant; "Mesh" indicates hernia repair using a mesh; "Matrix" signifies hernia repair with an acellularized 3D PLLA matrix; "Cell/Matrix" represents hernia repair using a cellularized 3D PLLA matrix; and "Cell/Matrix+Sec" indicates hernia repair using secretome-supplemented Cell/Matrix.
Abbreviations: PLLA: Poly-L-lactic acid; 3D: Three-dimensional.

Food and Drug Administration-approved material, commonly used in the manufacture of surgical sutures. PLLA-derived mesh is also available for hernia repair.[29] Nevertheless, synthetic, non-absorbable PP mesh is still preferentially used due to its low cost and durability, compared with PLLA-derived mesh, which tends to degrade over time. Complete resorption of PLLA monomers typically occurs within 6–24 months.[30] Our previous *in vitro* investigation showed that the PLLA/CC matrix lost approximately 30% of its mass after 24 weeks.[14] Meanwhile, present visual observation showed that the PLLA/CC matrix retained approximately 80% of its original dimensions after 2 months of sublay implantation *in vivo*. Given its biodegradable nature and relatively low mechanical strength, our PLLA/CC matrix may be less suitable as a sole therapy for securing IH injury.[14] Instead, this 3D device emerges as a potential adjuvant biomaterial to address the shortcomings of the present standard PP mesh, including pain, risks of infection, and adhesion to the implantation site, which also lacks regenerative capacity. In line with our previous work, this 3D PLLA/CC matrix is capable of carrying fibroblasts and facilitating their function in producing collagen.[12-14]

Upon incisional damage, the healing process of the abdominal wall fascia commences, wherein fibroblasts mediate the breakdown of "immature" COL3 into COL1 to initiate the development of high-integrity tissue. However, in the case of IH, abnormal healing occurs, and prolonged inflammation impairs this activity, leading to a lower ratio of COL1:COL3. A higher amount of COL3 results in ECM disorganization, thereby producing a weak abdominal wall with load-bearing failure.[24,25,31] This indicates that it is necessary to ensure not only increased collagen production, but also a higher ratio of COL1:COL3. In this study, we found that, when implanted adjacent to the incisional wound, our 3D cellularized matrix was associated with a substantial elevation of both total collagen and the COL1:COL3 ratio compared with the Sham and Mesh groups.

Effective blood perfusion is crucial during wound closure and is facilitated by the presence of mature blood vessels. While the inner compartment of a vessel is primarily composed of endothelial cells, mature vessels are characteristically ensheathed by vascular smooth muscle cells, indicated by the α-SMA marker.[32] Implantation of Cell/Matrix+Sec was associated with higher neovascularization counts and increased numbers of α-SMA-positive vessels. Notably, α-SMA-positive areas were also observed throughout the PLLA/CC matrix implant, which were absent in the PP mesh implant. This plausibly indicates the presence of myofibroblasts, a contractile α-SMA-positive phenotype of fibroblasts. During normal scar tissue development, fibroblasts differentiate into myofibroblasts. Due to their α-SMA expression, myofibroblasts generate mechanical forces that drive wound contraction and provide mechanical integrity.[24] However, in IH pathophysiology, fascial fibroblasts are likely to express a greater network of vimentin than actin, which is linked to significant ECM thinning in histologic sections of IH patient tissue.[33]

Moreover, a greater number of NSE-positive neuron bundles, which were stained to visualize neurons and neuroendocrine cells, were observed around the implant area in the Cell/Matrix+Sec group.[27] The ingrowth of neuron bundles throughout the Cell/Matrix+Sec implant suggests the development of highly specialized tissue to facilitate complete muscular activity. Accordingly, abdominal muscles implanted with Cell/Matrix+Sec also exhibited significantly stronger load-bearing capacity compared with the Sham group. Collectively, these findings demonstrate the capacity of Cell/Matrix+Sec to induce functional healing and regeneration of abdominal tissue in IH sublay repair, as evidenced by the formation of mature vessels and neural networks.

Interestingly, the supplementation of hUC-MSC Sec into the Cell/Matrix implant (Cell/Matrix+Sec group) was linked to

the most prominent results across all parameters. This finding suggests the vital role of Sec supplementation in fibroblast culture, as supported by our previous *in vitro* study, which demonstrated that hUC-MSC Sec can drive fibroblasts to synthesize a significantly higher amount of collagen.[13,14] In line with this, Hodge *et al.*[34] also highlighted that culturing fibroblasts in MSC Sec enhances cell proliferation and migration, due to the abundant growth factors contained in the Sec. Furthermore, adding MSC Sec during cell culture has been shown to induce cellular metabolic activity and upregulate gene expression of *HIF1A*, a master transcriptional regulator involved in cell survival and angiogenesis.[35] The rich repertoire of growth factors contained in hUC-MSC Sec may contribute to these findings. hUC-MSC Sec contains multiple growth factors, such as—but not limited to—VEGF, bFGF, human growth factor, and procollagen-I. These factors are known to play an interconnected role in wound healing by promoting fibroblast proliferation, migration, and function, ultimately leading to improved collagen deposition and epithelialization.[14] In addition, the Sec contains all secreted factors from MSCs, including exosomes and extracellular vesicles. Extracellular vesicles derived from MSCs alone have also shown therapeutic benefits in supporting wound healing by improving re-epithelization and collagen formation.[36-38]

To date, studies exploring the utilization of MSC-derived Sec for IH repair remain limited. Another application of MSC exosomes has been described, whereby the exosomes are conveyed in fibrin glue to fix the mesh implant at the hernia site. An *in vivo* study revealed that exosome/fibrin glue reduces the infiltration of pro-inflammatory macrophages surrounding the implant; however, both the expression and ratio of *COL1A1*:*COL3A1* genes were significantly lower compared with the control group.[39] In this study, we proposed the use of a 3D cellularized matrix with Sec supplementation for IH management. This fibroblast-seeded matrix can be shaped into desired dimensions with lightweight, highly porous, and dynamic properties, as opposed to conventional meshes, which are static and rigid in nature. Supplementation with Sec, due to its vast bioactive content, may stimulate fibroblasts to produce stronger scar tissue. Although the implant itself has a relatively lower mechanical strength compared with standard mesh,[14] when implanted sublay, our cellularized matrix achieved stronger tissue strength and better tissue maturation compared with PP mesh, suggesting its ability to promote innate tissue regeneration.

While this work presents the therapeutic potential of a cellularized matrix in promoting tissue regeneration following IH, further investigations are needed to address the limitations of the present study. Future studies should include larger cohorts to strengthen statistical power. Investigations into the optimal cell dosing and mechanisms of action should be conducted to support clinical translation. In addition, time-lapse observations of the tissue healing process and assessments of the long-term effects of the cellularized matrix implant are warranted. Nevertheless, the 3D cellularized matrix supplemented with Sec emerges as a promising adjuvant to present standard mesh management, especially in high-risk populations with altered regenerative capabilities.

5. Conclusions

Across this study, we displayed Cell/Matrix+Sec as a potential adjuvant implant for IH repair. Cell/Matrix+Sec is a 3D cellularized matrix with the supplementation of hUC-MSCs Sec. The 3D matrix template is made of PLLA/CC polymer, which enables attachment, growth, and fibroblasts function; while Sec supplementation, due to its vast growth factors content, is known to stimulate fibroblast functions. *In vivo* IH sublay implantation of Cell/Matrix+Sec results in better development of a functional tissue, further verified by the strong load-bearing capacity of the affected abdominal muscle as compared to sham and PP mesh-implanted groups.

Acknowledgement
We would like to thank drh. Permanawati, Sert.DHPHL, and Mrs. Suhartin, Amd, for their contributions and assistance in establishing the rat incisional hernia repair model.
Financial support
This study was funded by the Institute of Research and Community Service of Tarumanagara University (grant numbers: 0437-Int-KLPPM/UNTAR/V/2024; 070-SPK-PENREG-KLPPM/UNTAR/IV/2024) and supported by Baermed Tissue Engineering Ltd., Freienbach, Switzerland.
Conflicts of interest statement
HUB has an interest in acquiring intellectual properties in tissue engineering. Other authors declare no potential conflict of interest.
Author contributions
Conceptualization: SH and HUB; *Data curation*: SH, OM, and ES; *Formal analysis:* OM and AE; *Funding acquisition*: SH and HUB; *Investigation:* SH, OM, and AE; *Methodology:* SH, ES, and HUB; *Supervision*: SH, OM and HUB; *Writing – original draft:* SH and OM; *Writing – review & editing:* SH, OM, and HUB. All authors read and approved the final manuscript.
Ethics approval and consent to participate
The procedures used in this study were approved by the Human Research Ethics Committee of Tarumanagara University (UTHREC No. PPZ20192062). Fresh human umbilical cord was obtained from a healthy donor with parental consent. The animal study was conducted at the Tarumanagara Human Cell Technology Laboratory, Faculty of Medicine, Tarumanagara University, Jakarta, Indonesia, with approval from the Institutional Animal Care and Use Committee (IACUC) of Tarumanagara University (IACUC No. 017.KEPH/UPPM/FK/VI/2023).
Consent for publication
Not applicable.
Availability of data
Data are available from the corresponding author upon reasonable request.

References

1. Caglià P, Tracia A, Borzì L, *et al.* Incisional hernia in the elderly: Risk factors and clinical considerations. *Int J Surg.* 2014;12(S2):S164-S169. doi: 10.1016/j.ijsu.2014.08.357
2. Holihan JL, Hannon C, Goodenough C, *et al.* Ventral hernia repair: A meta-analysis of randomized controlled trials. *Surg Infect (Larchmt).* 2017;18(6):647-658. doi: 10.1089/sur.2017.029
3. Itatsu K, Yokoyama Y, Sugawara G, *et al.* Incidence of and risk factors for incisional hernia after abdominal surgery. *Br J Surg.* 2014;101(11):1439-1447.

doi: 10.1002/bjs.9600
4. Eker HH, Hansson BME, Buunen M, *et al.* Laparoscopic vs open incisional hernia repair. *JAMA Surg.* 2013;148(3):259-263. doi: 10.1001/jamasurg.2013.1466
5. van Silfhout L, Leenders LAM, Heisterkamp J, Ibelings MS. Recurrent incisional hernia repair: Surgical outcomes in correlation with body-mass index. *Hernia.* 2021;25(1):77-83. doi: 10.1007/s10029-020-02320-5
6. Thankam FG, Larsen NK, Varghese A, *et al.* Biomarkers and heterogeneous fibroblast phenotype associated with incisional hernia. *Mol Cell Biochem.* 2021;476(9):3353-3363. doi: 10.1007/s11010-021-04166-6
7. Peeters E, De Hertogh G, Junge K, Klinge U, Miserez M. Skin as marker for collagen type I/III ratio in abdominal wall fascia. *Hernia.* 2014;18(4):519-525. doi: 10.1007/s10029-013-1128-1
8. Hu W, Zhang Z, Zhu L, *et al.* Combination of polypropylene mesh and *in situ* injectable mussel-inspired hydrogel in laparoscopic hernia repair for preventing post-surgical adhesions in the piglet model. *ACS Biomater Sci Eng.* 2020;6(3):1735-1743. doi: 10.1021/acsbiomaterials.9b01333
9. Heymann F, von Trotha KT, Preisinger C, *et al.* Polypropylene mesh implantation for hernia repair causes myeloid cell-driven persistent inflammation. *JCI Insight.* 2019;4(2):e123862. doi: 10.1172/jci.insight.123862
10. Amato G, Puleio R, Romano G, *et al.* Physiologic cyclical load on inguinal hernia scaffold ProFlor turns biological response into tissue regeneration. *Biology (Basel).* 2023;12(3):434. doi: 10.3390/biology12030434
11. Garcia DPC, Santos Neto C, Hubner PNV, *et al.* Treatment of abdominal wall hernia with suture, or polypropylene, or collagen prosthesis. *Acta Cir Bras.* 2016;31(6):371-376. doi: 10.1590/S0102-865020160060000002
12. Hendrawan S, Bono E, Hutter A, Weber U, Lheman J, Baer HU. Evaluation of 3D PLLA scaffolds coated with nano-thick collagen as carrier for hepatocytes. *J Biomed Mater Res Part B Appl Biomater.* 2021;109(5):723-732. doi: 10.1002/jbm.b.34738
13. Hendrawan S, Lheman J, Weber U, *et al.* Fibroblast matrix implants-a better alternative for incisional hernia repair? *Biomed Mater.* 2024;19(3):035033. doi: 10.1088/1748-605X/ad3da4
14. Hendrawan S, Marcelina O, Tan ST, Baer HU. Immobilization of hUC-MSCs conditioned medium on 3D PLLA collagen-coated matrix enhances diabetic wound healing progression. *Eng Regen.* 2024;5(3):421-431. doi: 10.1016/j.engreg.2024.04.005
15. Hendrawan S, Kusnadi Y, Lagonda CA, *et al.* Wound healing potential of human umbilical cord mesenchymal stem cell conditioned medium: An *in vitro* and *in vivo* study in diabetes-induced rats. *Vet World.* 2021;14(8):2109-2117. doi: 10.14202/vetworld.2021.2109-2117
16. Tan ST, Aisyah PB, Firmansyah Y, Nathasia N, Budi E, Hendrawan S. Effectiveness of secretome from human umbilical cord mesenchymal stem cells in gel (10% SM-hUCMSC gel) for chronic wounds (diabetic and trophic ulcer) – phase 2 clinical trial. *J Multidiscip Healthc.* 2023;16:1763-1777. doi: 10.2147/JMDH.S408162
17. Tan ST, Firmansyah Y, Halim KC, Aisyah PB, Hendrawan S. Effectiveness of conditioned medium mesenchymal stem cells intracutaneous for trophic ulcer due to morbun hansen. *Bali Med J.* 2024;13(1):725-736. doi: 10.15562/bmj.v13i1.5022
18. Liao CJ, Chen CF, Chen JH, Chiang SF, Lin YJ, Chang KY. Fabrication of porous biodegradable polymer scaffolds using a solvent merging/particulate leaching method. *J Biomed Mater Res.* 2002;59(4):676-681. doi: 10.1002/jbm.10030
19. Sugiyama K, Okamura A, Kawazoe N, Tateishi T, Sato S, Chen G. Coating of collagen on a poly(l-lactic acid) sponge surface for tissue engineering. *Mater Sci Eng C.* 2012;32(2):290-295. doi: 10.1016/j.msec.2011.10.031
20. Chen G, Okamura A, Sugiyama K, *et al.* Surface modification of porous scaffolds with nanothick collagen layer by centrifugation and freeze-drying. *J Biomed Mater Res Part B Appl Biomater.* 2009;90(2):864-872. doi: 10.1002/jbm.b.31356
21. Melman L, Jenkins ED, Hamilton NA, *et al.* Early biocompatibility of crosslinked and non-crosslinked biologic meshes in a porcine model of ventral hernia repair. *Hernia.* 2011;15(2):157-164. doi: 10.1007/s10029-010-0770-0
22. Fuentes R, Saravia D, Arias A, Prieto R, Dias F. Mandibular dental implant placement using demineralized bone matrix (DBM). *Biomed Res.* 2017;28(6):2656-2660.
23. Liu J, Song Q, Yin W, *et al.* Bioactive scaffolds for tissue engineering: A review of decellularized extracellular matrix applications and innovations. *Exploration.* 2025;5(1):20230078. doi: 10.1002/EXP.20230078
24. Thankam FG, Palanikumar G, Fitzgibbons RJ, Agrawal DK. Molecular mechanisms and potential therapeutic targets in incisional hernia. *J Surg Res.* 2019;236:134-143. doi: 10.1016/j.jss.2018.11.037
25. Reilly MJ, Larsen NK, Agrawal S, Thankam FG, Agrawal DK, Fitzgibbons RJ. Selected conditions associated with an increased incidence of incisional hernia: A review of molecular biology. *Am J Surg.* 2021;221(5):942-949. doi: 10.1016/j.amjsurg.2020.09.004
26. Arenal JJ, Rodriguez-Vielba P, Gallo E, Tinoco C. Hernias of the abdominal wall in patients over the age of 70 years. *Eur J Surg.* 2002;168(8-9):460-463. doi: 10.1080/110241502321116451
27. Amato G, Agrusa A, Puleio R, Calò P, Goetze T, Romano G. Neo-nervegenesis in 3D dynamic responsive implant for inguinal hernia repair: Qualitative study. *Int J Surg.* 2020;76:114-119. doi: 10.1016/j.ijsu.2020.02.046
28. Amato G, Agrusa A, Calò PG, *et al.* Fixation free laparoscopic obliteration of inguinal hernia defects with the 3D dynamic responsive scaffold ProFlor. *Sci Rep.* 2022;12(1):18971. doi: 10.1038/s41598-022-23128-6
29. Tyler B, Gullotti D, Mangraviti A, Utsuki T, Brem H. Polylactic acid (PLA) controlled delivery carriers for biomedical applications. *Adv Drug Deliv Rev.* 2016;107:163-175. doi: 10.1016/j.addr.2016.06.018
30. Stefaniak K, Masek A. Green copolymers based on poly(lactic acid)-short review. *Materials (Basel).* 2021;14(18):5254. doi: 10.3390/ma14185254
31. Friedman DW, Boyd CD, Norton P, *et al.* Increases in type III collagen gene expression and protein synthesis in patients with inguinal hernias. *Ann Surg.* 1993;218(6):754-760. doi: 10.1097/00000658-199312000-00009
32. Zhang J, Nugrahaningrum DA, Marcelina O, *et al.* Tyrosol facilitates neovascularization by enhancing skeletal muscle cells viability and paracrine function in diabetic hindlimb ischemia mice. *Front Pharmacol.* 2019;10:909. doi: 10.3389/fphar.2019.00909
33. Diaz R, Quiles MT, Guillem-Marti J, *et al.* Apoptosis-like cell death induction and aberrant fibroblast properties in human incisional hernia fascia. *Am J Pathol.* 2011;178(6):2641-2653. doi: 10.1016/j.ajpath.2011.02.044
34. Hodge JG, Decker HE, Robinson JL, Mellott AJ. Tissue TissueE, Robinson JL, Melmesenchymal stem cell secretome capacity to improve regenerative activity of keratinocytes and fibroblasts *in vitro*. *Wound Repair Regen.* 2023;31(3):367-383. doi: 10.1111/wrr.13076
35. Kastner N, Mester-Tonczar J, Winkler J, *et al.* Comparative effect of MSC secretome to MSC co-culture on cardiomyocyte gene expression under hypoxic conditions *in vitro*. *Front Bioeng Biotechnol.* 2020;8:502213. doi: 10.3389/fbioe.2020.502213
36. Li Q, Li B, Ye T, *et al.* Requirements for human mesenchymal stem celll stem cellman mesenchymal stem cellndi*Interdiscip Med.* 2023;1(1):e20220015. doi: 10.1002/INMD.20220015
37. Zhong W, Meng H, Ma L, *et al.* Hydrogels loaded with MSC-derived small extracellular vesicles: A novel cell-free tissue engineering system

for diabetic wound management. *VIEW*. 2024;5(4):20230110. doi: 10.1002/VIW.20230110
38. Tian L, Wang Z, Chen S, *et al*. Ellagic acidic acidisEVs encapsulated in GelMA hydrogel accelerate diabetic wound healing by activating EGFR on skin repair cells. *Cell Prolif*. 2025:e70064. doi: 10.1111/cpr.70064
39. Blázquez R, Sánchez-Margallo FM, Álvarez V, Usón A, Marinaro F, Casado JG. Fibrin glue mesh fixation combined with mesenchymal stem cells or exosomes modulates the inflammatory reaction in a murine model of incisional hernia. *Acta Biomater*. 2018;71:318-329. doi: 10.1016/j.actbio.2018.02.014

Received: May 21, 2025
Revised: August 5, 2025
Accepted: August 6, 2025
Available online: September 4, 2025